Spectroscopic and dynamical studies of the S_1 and S_2 states of decatetraene in supersonic molecular beams

Hrvoje Petek, Andrew J. Bell, and Keitaro Yoshihara
Institute for Molecular Science, Myodaiji, Okazaki 444, Japan

Ronald L. Christensen
Department of Chemistry, Bowdoin College, Brunswick, Maine 04011

Fluorescence and fluorescence excitation spectra of *all-trans*-2,4,6,8-decatetraene have been obtained in free jets and in inert-gas clusters. In isolated decatetraene, excitation into $1\,^1B_u$ (S_2) results in emission from both S_2 ($1\,^1B_u \rightarrow 1\,^1A_g$) and S_1 ($2\,^1A_g \rightarrow 1\,^1A_g$) on time scales that are faster than the 10 ns experimental resolution. In clusters, rapid electronic and vibrational relaxation leads to long-lived (360 ns) emission from thermally relaxed levels of S_1. Direct excitation of low-lying, S_1 vibronic levels in cold, isolated molecules also results in long-lived $S_1 \rightarrow S_0$ fluorescence, as expected for this symmetry-forbidden transition. The detection of S_1 emission in free decatetraene has permitted the first detailed study of the vibronic structure and kinetics of the $2\,^1A_g$ state of an isolated, *all-trans* linear polyene. The $S_1 \leftarrow S_0$ fluorescence excitation spectrum is rich in low-frequency vibronic progressions. Analysis of this spectrum suggests that the transition not only is made allowed by vibronic coupling involving low-frequency b_u skeletal modes (Herzberg–Teller coupling), as for polyenes in condensed phases, but also gains intensity from interactions between the electronic motion and the hindered rotations (torsions) of the terminal methyl groups. Preliminary analysis suggests that the barriers to internal rotation of the methyl groups must be substantially reduced in the $2\,^1A_g$ (S_1) state. For isolated decatetraene, the $2\,^1A_g$ fluorescence lifetimes show a monotonic decrease with increasing vibrational energy, presumably due to increased mixing with the $1\,^1B_u$ state.

I. INTRODUCTION

The low-lying excited states of linear polyenes have been the subject of considerable experimental and theoretical activity in recent years.[1] These investigations, in large part, have been motivated by the roles of polyenes in several important photobiological processes, including energy transfer and photoprotection in photosynthesis and cis-trans photoisomerization in visual systems and photosynthetic bacteria. In addition, electronically excited polyenes undergo photoinduced cycloadditions and other pericyclic reactions.[2,3] Experimental work in these areas has been reinforced by a long-standing interest in developing better theoretical descriptions of one-dimensional, conjugated π electron systems. Polyenes provide many examples where the interactions between theory and experiment have led to a deeper understanding of excited-state electronic structures and chemical dynamics.

Much of the recent information about polyene electronic states has come from studies of model systems of intermediate length.[4–16] Optical experiments on simple polyenes with four or more conjugated double bonds have established the presence of a $2\,^1A_g$ (S_1) state between the ground state [$1\,^1A_g$ (S_0)] and first one-photon-allowed excited state [$1\,^1B_u$ (S_2)].[1] In condensed phases, absorption into the $1\,^1B_u$ state is typically followed by a red-shifted emission from $2\,^1A_g$, though the fluorescence yields are sensitive to details of molecular structure and environment. Thus octatetraene and longer polyenes have substantial $S_1 \rightarrow S_0$ fluorescence yields (e.g., $\Phi_f > 0.70$ for *all-trans* octatetraene in rigid glasses and mixed crystals),[4] whereas hexatriene and butadiene have vanishingly small emissions ($\Phi_f < 10^{-5}$). The lack of emission from shorter polyenes has made it difficult to establish the ordering of their lowest excited states, let alone the details of excited-state relaxation and photochemical pathways in these prototypical systems.

The striking contrast between the fluorescence properties of butadiene and hexatriene and those of the longer polyenes is most likely related to differences in the excited-state ($2\,^1A_g$ and $1\,^1B_u$) geometries of these molecules.[17,18] Although ethylene undergoes a 90° twist upon excitation from $1\,^1A_g$ to $1\,^1B_u$,[19] theoretical calculations[20,21] and modeling of resonance Raman and absorption spectra[22–25] indicate that the $1\,^1B_u$ states of butadiene and longer polyenes retain their planar, ground-state structures. In contrast, *ab initio* calculations on butadiene and hexatriene predict that the low-lying $2\,^1A_g$ state is nonplanar.[17,18] The $2\,^1A_g$ state in octatetraene apparently is planar but with a low barrier (~ 1400 cm^{-1}) to cis-trans isomerization.[26,27] Recent calculations by Zerbetto and Zgierski[17] show that distortions from planar geometries in $2\,^1A_g$ allow twisting modes of a_u and b_g symmetry to play important roles in $2\,^1A_g \rightarrow 1\,^1A_g$ internal conversion. This dramatically accelerates internal conversion in the shorter polyenes, thus accounting for the

quenching of fluorescence. Similar effects should enhance internal conversion from $1\ ^1B_u$ to $2\ ^1A_g$. A nonplanar $2\ ^1A_g$ state thus should promote the nonradiative relaxation of the initially excited $1\ ^1B_u$ state by internal conversion. For longer polyenes, more planar $2\ ^1A_g$ states result in slower rates of $S_1 \rightarrow S_0$ internal conversion, allowing fluorescence to compete with other decay channels.

Even though polyenes longer than hexatriene fluoresce, simple model systems have not been extensively studied. This, in part, is due to the fact that they are not commercially available and are difficult to synthesize and purify in the amounts required to carry out extensive vibrational and electronic studies, particularly in molecular beams. Certain natural products, most notably derivatives of the visual chromophore retinal and longer polyenes such as β-carotene, are available and have received a great deal of experimental attention.[1,16] However, the relative complexity of these systems often prohibits detailed theoretical analysis and their low vapor pressures have precluded studies under isolated, collision-free conditions.

Short diphenylpolyenes, on the other hand, are both stable and highly fluorescent and thus amenable to detailed spectroscopic and kinetic studies.[28–40] *Cis-* and *trans*-stilbenes have been extensively studied by time-resolved optical experiments in solutions, in inert-gas clusters, and as isolated molecules.[30–32,39–41] These experiments have followed the *cis-trans* photoisomerization on short time scales (10^{-9}–10^{-13} s) and have provided detailed information on how electronic excitation is directed toward photochemical channels on excited-state potential surfaces. Ultrahigh-resolution, rotationally resolved fluorescence excitation spectra of *trans*-stilbene and diphenylbutadiene in molecular beams have revealed structural changes following electronic excitation.[42] The ability to study the spectroscopy and photochemistry of clusters in supersonic beams also has allowed investigation of solvation effects on cis-trans isomerization in the phenyl-substituted systems.

For diphenylbutadiene and longer diphenyl polyenes, the forbidden $2\ ^1A_g \leftarrow 1\ ^1A_g$ transition is below the optically allowed $1\ ^1B_u \leftarrow 1\ ^1A_g$ transition. The spectroscopy of these systems thus has much in common with that of unsubstituted analogs. However, the comparison of fluorescence yields reminds us that phenyl substituents have striking effects on the photophysical properties of polyenes, and it would not be surprising if the photochemistries were similarly affected. It thus will be important to extend the experiments on the diphenylpolyenes to unsubstituted polyene systems.

Two recent studies have opened the way to more-detailed experimental investigations of the spectroscopy and photochemistry of the intermediate length, unsubstituted polyenes. Buma, Kohler, and Song[43] have used multiphoton ionization techniques to obtain the excitation spectrum of the $2\ ^1A_g \leftarrow 1\ ^1A_g$ transition in several supersonically cooled *cis*-trienes. Extension of these experiments to *trans*-trienes (which have a much weaker $2\ ^1A_g \leftarrow 1\ ^1A_g$ oscillator strength) and dienes would circumvent the problems imposed by the lack of emission in these short polyenes. Parallel to the multiphoton ionization experiments on the trienes, Bouwman *et al.*[15] have reported emissions from the S_1
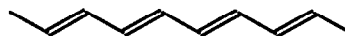
2,4,6,8-decatetraene

FIG. 1. *All-trans*-2,4,6,8-decatetraene.

($2\ ^1A_g$) and S_2 ($1\ ^1B_u$) states of several simple tetraenes and pentaenes, both as static gases and in supersonic jets. Previous gas-phase experiments on octatetraene indicated emission solely from the S_2 ($1\ ^1B_u$) state,[8,11] while in condensed phases rapid electronic and vibrational relaxation results in emission only from the S_1 ($2\ ^1A_g$) state.[5–8] The discovery of $2\ ^1A_g \rightarrow 1\ ^1A_g$ emissions from isolated polyenes and the development of improved synthetic procedures means that the structures and dynamics of the $2\ ^1A_g$ states of longer polyenes now can be studied in supersonic expansions with and without solvent perturbations. We report here on the dual emissions ($1\ ^1B_u \rightarrow 1\ ^1A_g$ and $2\ ^1A_g \rightarrow 1\ ^1A_g$) following excitation of the $1\ ^1B_u$ state, the one-photon, $2\ ^1A_g \leftarrow 1\ ^1A_g$ fluorescence excitation spectrum, and the single vibronic level decay kinetics of isolated decatetraene (Fig. 1). These results form the basis for more-detailed investigations of the spectroscopy and dynamics of $2\ ^1A_g$ states in several intermediate-length polyenes.

II. EXPERIMENT

All-trans-2,4,6,8-decatetraene was prepared from the Wittig reaction between hexadienal (Aldrich) and crotyltriphenylphosphonium bromide ("Instant Ylide"; Fluka). Ten grams of the latter was dissolved in 20–30 mL of dry tetrahydrofuran and the solution was stirred for 15 min; 3.3 mL of hexadienal was then added in a dropwise fashion to the reaction flask, which was held in an ice bath. After 10 min the reaction was quenched in a 10% NaOH solution and the aqueous layer was discarded. The decatetraene reaction mixture was then extracted into warm hexane and chromatographed on alumina or silica gel columns, using hexane as the eluting solvent. Crystalline decatetraene (mp of 137–139 °C) was obtained by precipitation from concentrated hexane solutions. Typical yields after the first recrystallization were > 50%. Crystalline samples stored in sealed vials at − 20 °C were stable for several months.

The apparatus for measuring fluorescence excitation and emission spectra of molecules in molecular beams under isolated conditions and in clusters has been described previously.[44] Briefly, the experimental setup consists of (i) a molecular-beam machine, (ii) an excimer-pumped dye laser excitation source, and (iii) emission detection optics and electronics.

A molecular beam of decatetraene was prepared by placing 10–50 mg of *all-trans*-decatetraene in a trough on the bottom flange next to the orifice of the pulsed molecular-beam valve, heating the sample to 50–80 °C to achieve sufficient vapor pressure, seeding it in a carrier gas, and expanding it through the 0.5 mm orifice of the pulsed valve during the 300–400 μs opening of the nozzle. In some cases higher

sample temperatures were used, though this generally was avoided due to accelerated polymerization of samples at higher temperatures. Decatetraene was studied as a free molecule by coexpanding the sample with up to 3000 Torr of He or in Ar clusters by replacing the He carrier gas with up to 3000 Torr of Ar. In He expansions, there was no evidence of He-decatetraene clusters or decatetraene aggregates. However, Ar_n:decatetraene cluster formation occurred above ~300 Torr of Ar stagnation pressure. At higher Ar pressures, the $S_2 \leftarrow S_0$ origin underwent a considerable red-shift due to increasing solvation by Ar. The actual cluster composition could not be determined with the present apparatus.

The excitation source for fluorescence measurements was an excimer-pumped dye laser (Lambda-Physik 104/2003). The second harmonic of Rhodamine 6G and the fundamental of p-terpheryl dye lasers were used to excite the S_2 and S_1 states, respectively. The bandwidth of the dye laser was ~0.3 cm^{-1}, the pulse width ~10 ns, and the repetition rate 10 Hz for fluorescence excitation spectroscopy and 30 Hz for emission spectroscopy. The excitation intensity was carefully controlled with neutral density filters in case of S_2 state excitation in order to avoid saturation of the strongly allowed transition. The dye laser wavelength was calibrated by measuring the optogalvanic spectrum of a neon hollow-cathode lamp.

The laser beam crossed the molecular beam 7–15 mm from the pulsed valve orifice. It was verified that the spectrum and the emission lifetimes did not depend on the nozzle-to-laser beam distance, indicating that at the point of interaction the sample had reached its terminal temperature and that collisions did not occur on the time scale of the measurements. This is crucial due to the long lifetimes of the S_1 state. The focusing of the laser beam was adjusted for excitation of the maximum number of molecules in the observation region, without saturating the transition.

The fluorescence was collected with $f/1$ optics and focused onto a Hamamatsu Photonics H3177 photomultiplier for fluorescence excitation spectra or onto the slit of a 250 mm monochromator for resolved emission spectra. For $S_2 \leftarrow S_0$ excitation spectra, fluorescence from either the S_2 or S_1 states could be recorded by placing appropriate optical filters in front of the photomultiplier tube (PMT). The PMT signal was integrated by a Stanford Research Systems boxcar integrator (SR-250), and the integrated value averaged and stored in a microcomputer. Simultaneously, the power of the excitation laser was monitored by a photodiode, whose signal was integrated with another channel of the boxcar, and the output was used to normalize the excitation spectra. The fluorescence excitation spectra generally were obtained by averaging the signal obtained from 10 excitation pulses for each 0.3 cm^{-1} scan interval.

In order to record emission spectra, the fluorescence was dispersed with a 590 lines/mm grating blazed at 300 nm (used in first order). The spectra were recorded with a 700 channel PAR 1420 optical multichannel analyzer (OMA). The resolution of the measured spectra (30 cm^{-1}) was limited by the 4 channel (100 μm) effective resolution of the OMA. The spectra were integrated for up to 10 min at a 30 Hz excitation rate.

Decatetraene - Emission spectrum upon excitation of S_2 origin
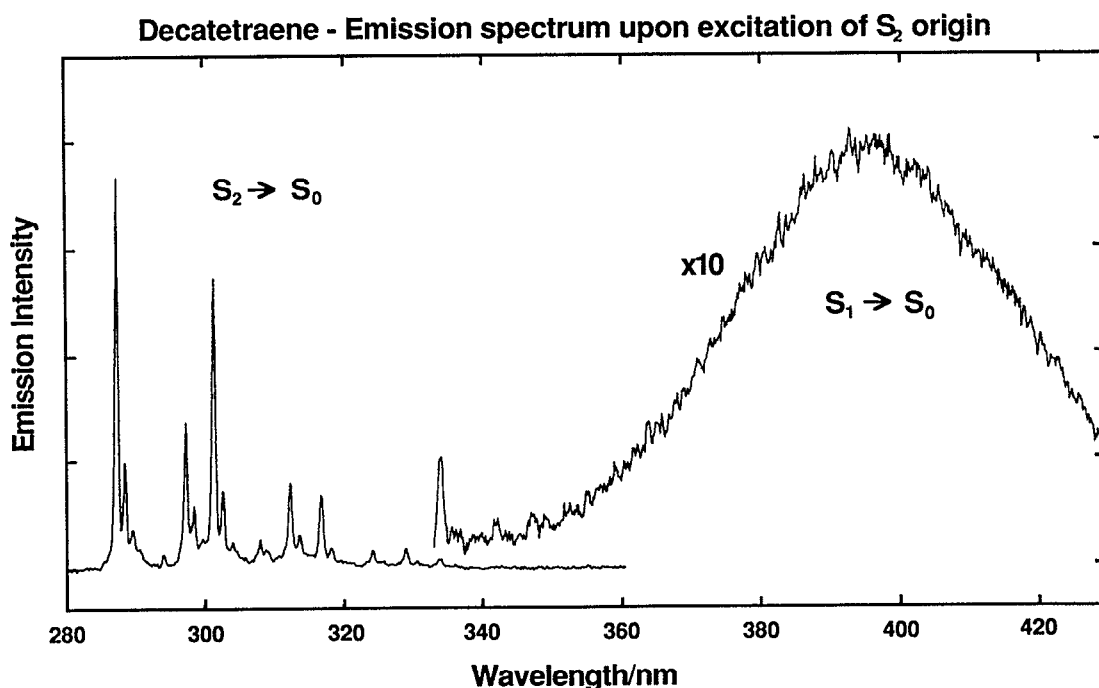
FIG. 2. 2 $^1A_g \to 1\ ^1A_g$ fluorescence of all-trans-decatetraene in a free jet following excitation of 1 $^1B_u \leftarrow 1\ ^1A_g$ electronic origin (287.49 nm). (Resolution = 60 cm^{-1}.)

III. RESULTS AND DISCUSSION

A. Dual fluorescence following $S_2 \leftarrow S_0$ excitation of isolated decatetraene

The emission spectrum obtained upon excitation of the $S_2 \leftarrow S_0$ electronic origin (287.49 nm) of isolated, jet-cooled decatetraene is given in Fig. 2. This spectrum reveals two distinct transitions: a well-resolved emission with an electronic origin coincident with the (0–0) of the $S_2 \leftarrow S_0$ absorption, and an unstructured emission at longer wavelengths. The structured fluorescence is assigned to $S_2 \rightarrow S_0$ ($1\,^1B_u \rightarrow 1\,^1A_g$) emission from the electronic origin of $1\,^1B_u$. This emission shows a close mirror-image relationship with the previously published $S_2 \leftarrow S_0$ fluorescence excitation spectrum.[15] The emission spectrum is dominated by 1190 and 1650 cm^{-1} modes which are assigned to totally symmetric carbon–carbon single-bond and carbon–carbon double-bond stretches. The relative dominance of the electronic origin indicates that, as with other long polyenes, the geometries of the $1\,^1B_u$ and $1\,^1A_g$ states are rather similar. In addition to the typically strong, carbon–carbon stretching modes, we also observe low-frequency modes at 150 and 290 cm^{-1} which can be assigned to a_g in-plane angle deformations. Similar modes have been observed in the $1\,^1B_u$ states of jet-cooled octatetraene (197 and 348 cm^{-1}) (Refs. 8 and 9) and decatetraene (132 and 273 cm^{-1}),[15] though this is the first instance where these low-frequency features have been observed for the $1\,^1A_g$ state in a free jet.

The broad, unstructured fluorescence previously had been assigned[15] as $S_1 \rightarrow S_0$ ($2\,^1A_g \rightarrow 1\,^1A_g$) emission from highly vibrationally excited states of S_1 that are isoenergetic and strongly coupled with the zero-point vibrational level of S_2 ($1\,^1B_u$). The spectral envelope is rather similar to that of $S_1 \rightarrow S_0$ emission from vibrationally relaxed decatetraene.[5] The displacement of the Franck–Condon maximum from the origin can be ascribed to differences in the C–C and C = C bond orders in the $2\,^1A_g$ and $1\,^1A_g$ states.

The relative intensities of the two emissions were found to be independent of the laser power, nozzle temperature, He stagnation pressure, and the distance between the nozzle and the point where the laser intersects the molecular beam. In addition, identical $S_2 \leftarrow S_0$ fluorescence excitation spectra were obtained when separately monitoring the two emissions. We thus must conclude that both emissions are from isolated decatetraenes excited to S_2 vibronic states, and in particular that the broad emission is not due to the formation of dimers or excimers in the molecular beam, nor due to absorption to spectroscopically distinct S_2 and S_1 vibronic states.

These results support our previous interpretation of the dual emissions observed in room-temperature, static gas samples of decatetraene and several other polyenes.[15] The ratio of the two emissions in the free jet is comparable to that observed for the static, room-temperature gas ($S_1 \rightarrow S_0 / S_2 \rightarrow S_0 = 0.7 \pm 0.2$).[15] This is somewhat surprising given the rather different S_2 vibronic states accessed in the jet and static vapor experiments, but consistent with the observation of identical $S_2 \leftarrow S_0$ excitation spectra when monitoring either S_2 or S_1 emission. Preliminary measure-

ments of lifetimes indicate < 10 ns decay times for both emissions. The $S_2 \leftarrow S_0$ vibronic linewidths have been used to estimate a 0.25 ps lifetime for the zero-point level of $1\,^1B_u$.[15] This suggests < 10^{-4} fluorescence yields for both $1\,^1B_u$ and $2\,^1A_g$ which is not unexpected given the 5762 cm^{-1} of excess energy (the $S_2 - S_1$ energy difference) in the initially excited states. More-accurate estimates of lifetimes and quantum yields await further study.

B. Fluorescence following $S_2 \leftarrow S_0$ excitation of decatetraene/Ar clusters

We have also studied the fluorescence excitation and emission spectra of decatetraene in Ar clusters. The $S_2 \leftarrow S_0$ fluorescence excitation spectra shift to the red with increasing argon stagnation pressure (> 1700 cm^{-1} at $P_{Ar} = 2$ atm), reflecting the growth in the Ar solvation shell. At high stagnation pressures of argon (~ 2 atm), complete solvation of decatetraene in large Ar clusters results in rapid electronic and vibrational relaxation. The emission is solely from the relaxed S_1 state giving a spectrum (Fig. 3) comparable to those obtained in low-temperature glasses.[5] The Franck–Condon envelopes of these spectra correspond well with the broad, red-shifted emission observed for isolated molecules and lend further support to the assignments discussed above. The fluorescence from argon clusters, though broad, shows sufficient vibronic detail to allow the assignment of the electronic origin ("false origin") at 347.6 nm. As expected for forbidden transitions, the corresponding solvent shifts of the $S_1 \leftrightarrow S_0$ spectra are considerably smaller than for the $S_2 \leftrightarrow S_0$ transitions.[1,12]

Spectra obtained at lower argon pressures show dual emissions, indicating partitioning between complexed and uncomplexed decatetraene. At higher stagnation pressures the S_2-state emission vanishes, and the $S_1 \rightarrow S_0$ emission grows progressively stronger. This suggests that the fluorescence excitation spectra are dominated by the more fluores-

Decatetraene $S_1 \rightarrow S_0$ Emission Spectrum in Ar Clusters
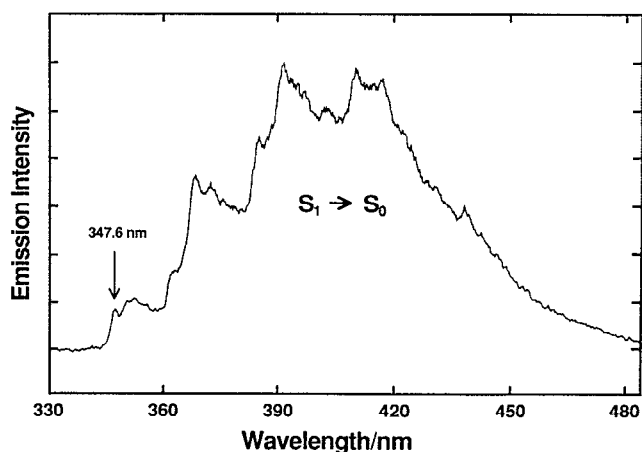
FIG. 3. $2\,^1A_g \rightarrow 1\,^1A_g$ fluorescence of *all-trans*-decatetraene in argon clusters following $S_0 \rightarrow S_2$ ($1\,^1A_g \leftarrow 1\,^1B_u$) excitation. (Instrumental resolution = 30 cm^{-1}.)

cent, complexed species and that these clusters (along with free decatetraene) have similar, Stokes-shifted, $S_1 \rightarrow S_0$ emission spectra. For larger clusters, decatetraene relaxation is complete and the effective temperature is lower, resulting in the increased resolution of the $S_1 \rightarrow S_0$ emission at high argon pressures (>2 atm). The $S_1 \rightarrow S_0$ fluorescence lifetimes also are sensitive to cluster size with lower pressures of argon giving shorter, nonexponential decay times. The broader $S_1 \rightarrow S_0$ fluorescence spectra indicate that these samples are considerably warmer than those formed at high stagnation pressures, either because the Ar cluster bath is so small that $S_2 \rightarrow S_1$ relaxation results in significant heating of the clusters, or because the clusters dissociate before decatetraene has fully vibrationally relaxed. These experiments indicate that the partitioning between $S_2 \rightarrow S_0$ and $S_1 \rightarrow S_0$ emissions can be controlled by the argon/decatetraene stoichiometry and that several argons are required to relax the excited decatetraene into the zero-point vibrational level of S_1. These observations also are consistent with rapid, nonradiative decay of S_1 decatetraene with high excess vibrational energies.

We thus focus on clusters in the "high-pressure" limit ($P_{Ar} > 2$ atm), where the decatetraene fluorescence appears to be insensitive to cluster-size. In this limit the fluorescence is well described by single-exponential kinetics with a decay time of 360 ns. This, the longest emission lifetime observed in

a linear polyene, confirms that the fluorescence is symmetry forbidden, as expected for the $2\,^1A_g \rightarrow 1\,^1A_g$ transition of an *all-trans* polyene (*cis* isomer impurities would have considerably shorter S_1 lifetimes due to loss of the inversion center). Previous measurements[5] of fluorescence lifetimes and quantum yields of *all-trans*-decatetraene in isopentane at room temperature ($\tau_f = 5$ ns, $\phi_f = 0.01$) and at 77 K ($\tau_f = 100$ ns, $\phi_f = 0.2$) indicate an intrinsic radiative lifetime of ~ 500 ns. Comparison between solution, cluster, and isolated molecule lifetimes is complicated by differences in quantum yields and in the $1\,^1B_u$–$2\,^1A_g$ energy separation (and expected differences in intensity borrowing through vibronic mixing[1]) in different solvent environments. Nevertheless, the 360 ns lifetime suggests a large fluorescence yield (0.5–1.0) for the decatetraene/argon clusters.

C. $2\,^1A_g \leftarrow 1\,^1A_g$ fluorescence excitation spectrum of isolated decatetraene

Figure 4 gives the free-jet, $S_1 \leftarrow S_0$ fluorescence excitation spectrum of decatetraene in the 1350 cm^{-1} region above the apparent "origin" at ~ 344.57 nm. An expanded view of the vibronic levels of this transition is given in Fig. 5. The most striking feature of the spectrum is the rich, rather complicated development of low-frequency vibronic bands, particularly the splitting of most bands into triplets. The free-jet
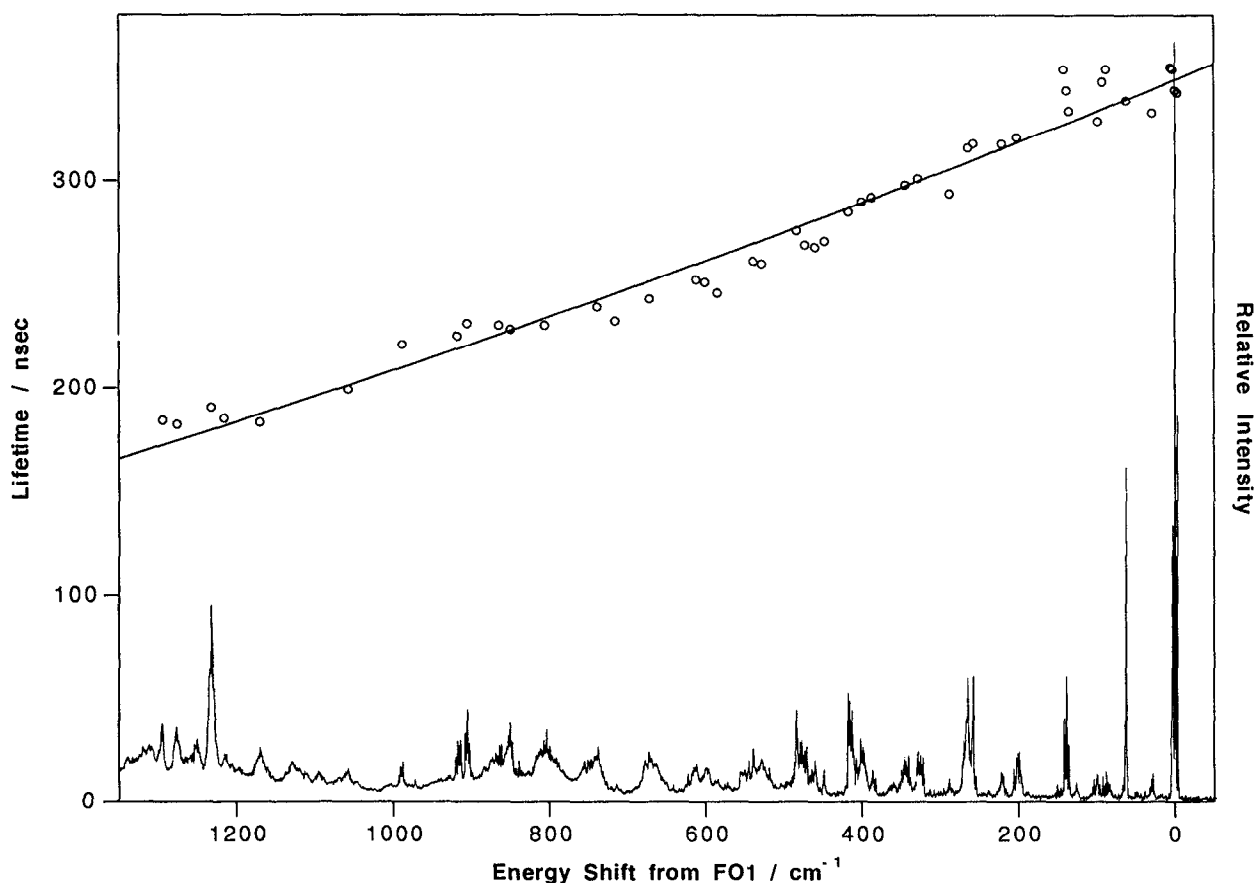
FIG. 4. $2\,^1A_g \leftarrow 1\,^1A_g$ fluorescence excitation spectrum and single vibronic level fluorescence lifetimes of *all-trans*-decatetraene in a free jet (0–1350 cm^{-1}). Fluorescence lifetimes are fit to a simple vibronic coupling model, $\tau = (\Delta E / \Gamma)^2$ (see text).

excitation spectrum of decatetraene thus contrasts previous, condensed-phase polyene spectra in which the $2\,^1A_g \leftarrow 1\,^1A_g$ transitions are dominated by combinations of high-frequency, carbon–carbon stretching modes.[1,6,7,13,14] Tentative assignments of the most prominent, low-energy $S_1 \leftarrow S_0$ vibronic features are provided in Table I. Also included in this table are the fluorescence lifetimes of most of the vibronic bands.

The excitation spectrum is complicated by the symmetry-forbidden nature of the transition which requires that vibronic intensity be built on "false" origins. Analysis of the $S_1 \leftarrow S_0$ absorption in decatetraene thus rests on the correct identification of the false origins and an understanding of the mechanisms by which the transition is made allowed. Pre-

vious high-resolution absorption and emission experiments on several model polyenes (including decatetraene) in mixed crystals provide useful guides.[1,6,13,14,45,46] Under conditions (site symmetries) that preserve the g and u symmetry labels, polyene $2\,^1A_g \leftrightarrow 1\,^1A_g$ spectra exhibit the classic patterns of Herzberg–Teller vibronic coupling. The spectra are characterized by forbidden origins with spectral intensities being built on low-frequency b_u vibrations which induce mixing between the $2\,^1A_g$ and $1\,^1B_u$ electronic states. Previous work on the fluorescence excitation spectra of decatetraene in 4.2 K n-undecane leads to the identification of a 72 cm^{-1} Herzberg–Teller promoting mode in the $2\,^1A_g$ state.[5] A similar mode has been observed in octatetraene[46] with the lower reduced mass resulting in a somewhat higher frequen-
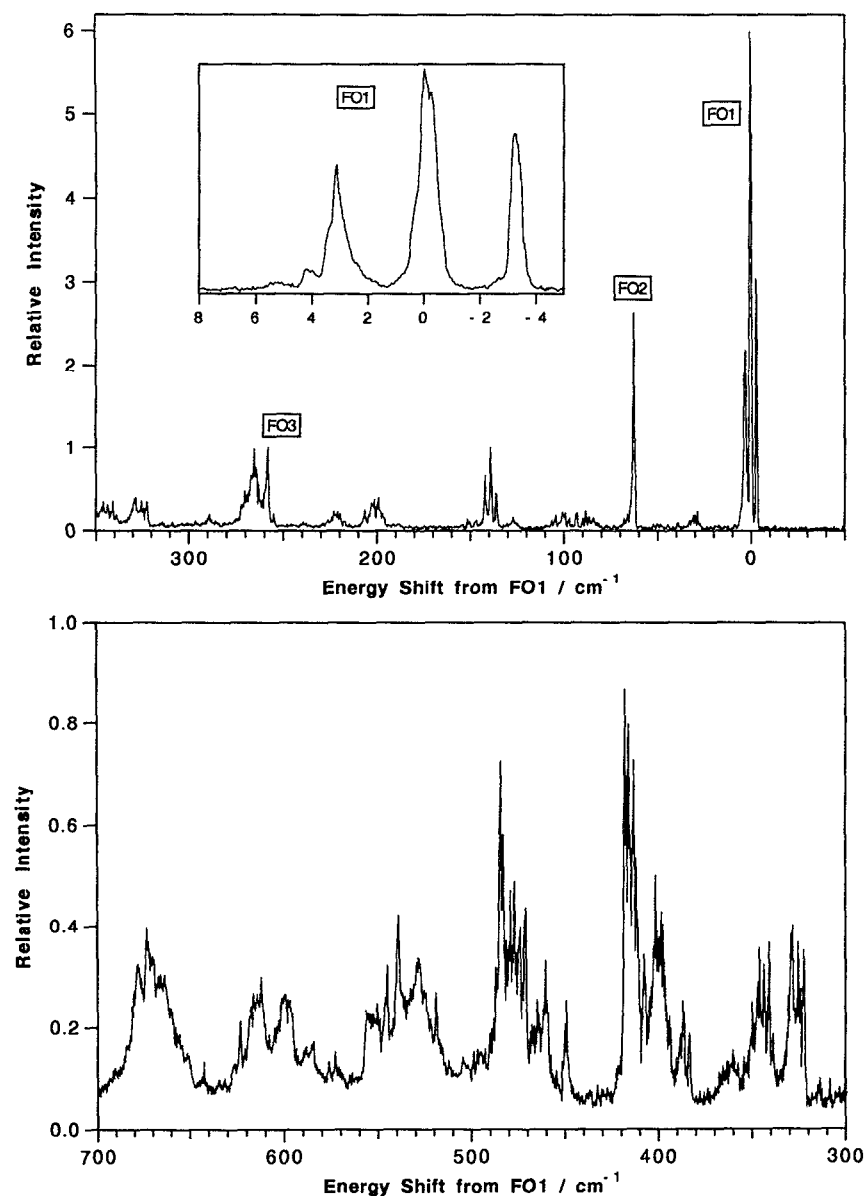
FIG. 5. Expanded views of low-energy vibronic transitions in the $2\,^1A_g \leftarrow 1\,^1A_g$ fluorescence excitation spectrum of *all-trans*-decatetraene in a free jet. Note that the expanded intensity scales of the lower panels. The inset gives an expanded view of false origin 1 (FO1) at a stagnation pressure of 4000 Torr helium and a laser step size of 0.04 cm^{-1}.
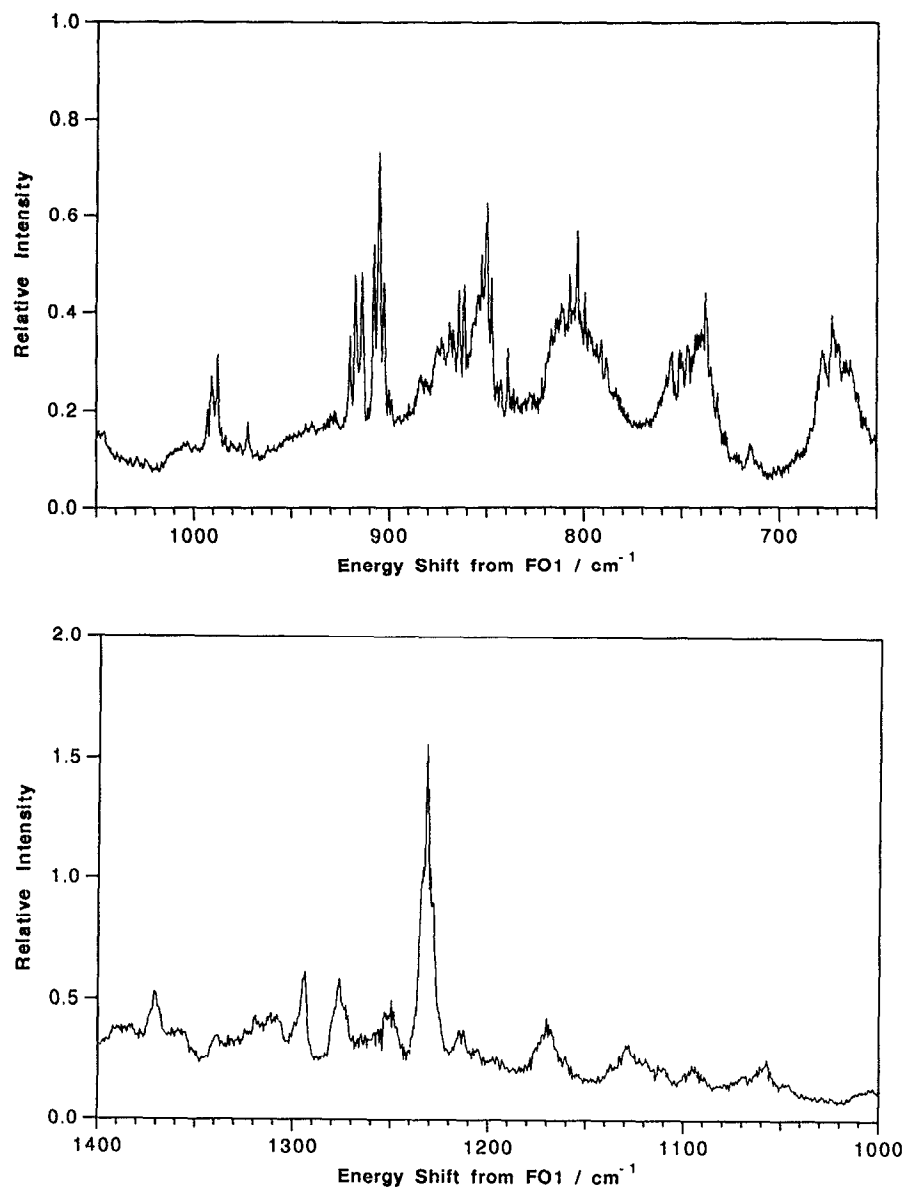
FIG. 5. (*Continued*).

cy (93 cm^{-1}). Normal-mode calculations on these systems identify the low-frequency vibrations as b_u in-plane skeletal bends of the polyene chain.[47–49] The analysis of the excitation spectrum of isolated decatetraene indicates an analogous low-frequency promoting mode ($\nu_{HT} \geqslant 65$ cm^{-1}) that is identified as "false origin 2" (FO2) in Table I. This mode plays an important (though by no means dominant) role in the low-frequency vibronic development of the $2\,^1A_g \leftarrow 1\,^1A_g$ transition and also is seen in combination with the 1232 cm^{-1}, carbon–carbon single-bond-stretching mode. Vibronic transitions built on FO2 typically appear as sharp, well-defined "singlets." Our inability to observe the symmetry-forbidden electronic origin (0–0) precludes a more-accurate measurement of the frequency of this vibration, though, as will be seen below, there are reasons to estimate an upper bound of 70 cm^{-1}, in good agreement with the b_u

mode observed in the decatetraene/undecane mixed crystal.[5]

Assignment of the other major false origin system ("false origin 1"; FO1 in Table I) for isolated decatetraene is not as straightforward. The lowest-energy feature in the $2\,^1A_g \leftarrow 1\,^1A_g$ excitation spectrum consists of a "triplet" of peaks at 29 019, 29 022, and 29 025 cm^{-1} with the triplet showing indications of additional fine structure (see inset of Fig. 5.). This triplet pattern is repeated for most of the other bands in the spectrum. The additional fine structure could not be fully resolved in our experiment (due to a limiting resolution of 0.3 cm^{-1}) and most likely is due to rotational P and R branch envelopes. We have identified the low-energy triplet of peaks (the strongest bands in our spectrum) as a false origin that is induced by coupling between the electronic motion and the hindered rotation of the terminal

TABLE I. Band maxima in the free-jet $2\,^1A_g \leftarrow 1\,^1A_g$ fluorescence excitation spectrum of *all-trans*-2,4,6,8-decatetraene.

Frequency (cm^{-1})[a]	Assignment	Lifetime (ns)
0 (29 022 cm^{-1}) (b_u)[b]	FO1	344
63 (b_u)	FO2	339
139 (a_g)	FO1 + 139	344
203 (a_g)	FO1 + 203	321
223 (a_g)	FO1 + 223	318
259 (b_u)	FO3	318
266	FO2 + 203	316
329 (a_g)	FO1 + 329 (FO2 + 266)	301
342	FO1 + 139 + 203	298
387	FO2 + 329	292
400	FO3 + 139	290
416 (a_g)	FO1 + 416	285
461	FO3 + 203	271
474	FO2 + 416	269
484[c]	FO1 + 2(139) + 203/FO3 + 223	276
529[c]	FO1 + 203 + 329	260
539[c]	FO3 + 2(139)/FO1 + 139 + 2(203)	261
601[c]	FO3 + 139 + 203	251
613[c]	FO3 + 139 + 223/FO1 + 203 + 416	252
673[c]	FO1 + 2(139) + 2(203)/FO3 + 3(139) (FO2 + 203 + 416)	243
740[c]	FO1 + 139 + 3(203)/FO3 + 2(139)/ FO1 + 329 + 416	239
804 (a_g)	FO1 + 804	230
806[c]	FO1 + 3(139) + 2(203)/FO3 + 4(139) (FO2 + 139 + 203 + 416)	
850 (a_g)	FO1 + 850	228
852[c]	FO1 + 2(139) + 3(203)/FO3 + 3(139) + 203	
905 (a_g)	FO1 + 905	231
988 (b_u?)	FO4(?)	221
1232 (a_g, C–C)	FO1 + 1232	190
1294	FO2 + 1232	184

[a] Frequencies of peaks are measured relative to the band maximum of false origin 1 (FO1 has an absolute value of 29 022 cm^{-1}.) The precise location of the electronic origin (0–0) is not known. For purposes of simplification, only the maxima of each set of "triplets" is given in this table.

[b] Denotes symmetry of vibrations, assuming that $2\,^1A_g$ is described by the C_{2h} point group. As noted in the text, some a_g vibrations may involve double quanta or combinations of nontotally symmetric normal modes (e.g., a_u or b_g).

[c] These bands are broad and most likely are due to the overlap of two or more of the combination bands indicated in the table.

methyl groups. Such couplings have not previously been invoked in discussions of polyene spectra. However, there is ample precedence for this effect in the supersonic jet spectra of several methyl-substituted benzenes[50–53] and fluorotoluenes.[54] The spectra of these molecules are characterized by an analogous fine structure, typically within 100 cm^{-1} of the $S_1 \leftrightarrow S_0$ electronic origins, that can be assigned to transitions associated with the internal rotation of the ring methyl groups. Furthermore, these spectra can be accounted for quantitatively by changes in the barriers to rotation in going from the ground to excited electronic states.[53,54] Of particular interest are the experiments of Ito and co-workers on the electronic spectroscopy of jet-cooled 1,3,5-trimethylbenzene (mesitylene).[50,51] Mesitylene, like decatetraene, has a symmetry-forbidden $S_1 \leftarrow S_0$ transition and the 0–0 band thus does not appear in the spectrum. A triplet of low-frequency bands appears on the high-energy side of the forbidden 0–0, suggesting strong coupling between the electronic motion

and methyl internal rotation. Totally symmetric vibrations form progressions on the low-frequency triplet as well as on a second, vibronically induced (Herzberg–Teller coupling) false origin for which a single, sharp peak is observed. The two sets of bands in the electronic spectrum of mesitylene thus are remarkably similar to the progressions we have assigned to the two false origins in isolated decatetraene.

The appearance of methyl torsional fine structure in the free-jet spectra of substituted benzenes is due to the modest barriers to internal rotation in the ground and excited states of these systems.[53,54] Indeed, in molecules such as toluene where methyl groups are bonded to a framework of twofold symmetry, the energy levels associated with rotation are essentially those of a free rotor.[55] This gives rise to the extended (10–200 cm^{-1}) methyl torsional structure seen in the free-jet $S_1 \leftarrow S_0$ spectra of the methyl-substituted benzenes.[50–53] In decatetraene, we also observe some complex clumps of weak transitions within 100 cm^{-1} of FO1. These

also may be associated with methyl torsions. However, the data on short *trans*-polyenes such as propene,[56] isoprene,[57] and 1,3-pentadiene[58] indicate that these molecules have large (600–700 cm^{-1}) ground-state barriers to methyl rotation. The resulting ground-state tunneling splittings thus are too small to detect in our experiments. The appearance of fine structure in the $S_1 \leftarrow S_0$ transition of decatetraene would require a reduction of the rotational barriers in the 2 ^1A_g state to < 200 cm^{-1}.[53,55]

A significant reduction in the barrier to methyl rotation in the 2 ^1A_g state of decatetraene might be due to a combination of the following: (i) *Decreased repulsions* between the π-symmetry orbitals on the CH$_3$ groups (π_{CH_3}) and the π orbitals on the terminal C=C bonds ($\pi_{C=C}$) due to the predicted bond-order inversion between C=C and C–C bonds in going from the ground state to 2 ^1A_g. Such rearrangements are predicted by theory[49,59–62] and are indicated by the extended Franck–Condon envelopes seen in the $S_1 \rightarrow S_0$ emission spectrum in the Ar clusters (Fig. 3). (ii) *Attractive interactions* between the vacant $\pi^*_{CH_3}$ and $\pi^*_{C=C}$ orbitals.[63] If the fine structure seen in the $S_1 \leftarrow S_0$ excitation spectrum is due to hindered rotation, then the electronic origin (0–0) must lie within a few cm^{-1} of the lowest energy feature at 29 019 cm^{-1}. For the purposes of this paper, we have arbitrarily assigned the most-intense spectral feature in the lowest-energy triplet (29 022 cm^{-1}) as the zero of vibronic energy in 2 ^1A_g (see Table I). It should be stressed, however, that the precise location of the electronic origin has not been determined at this time.

Another possibility to consider is that the triplet of peaks centered at 29 022 cm^{-1} is due to a second b_u Herzberg–Teller promoting vibration that is merely modulated by the methyl rotations. However, previous experiments and normal-mode calculations on molecules such as octatetraene and decapentaene (reduced mass comparable to that of decatetraene) argue against this assignment. Four b_u promoting modes (93, 463, 538, and 1054 cm^{-1}) have been identified in the 2 $^1A_g \leftarrow 1$ ^1A_g mixed-crystal spectrum of octatetraene.[46] These frequencies are reasonably well accounted for by theory,[47–49] which predicts corresponding modes at lower frequency in molecules such as decapentaene (62, 282, 497, and 553 cm^{-1} in 1 ^1A_g) and decatetraene.[47] It thus would be difficult to rationalize two b_u promoting vibrations separated by 63 cm^{-1}, since one of these must be the counterpart of the lowest-frequency b_u modes that play such dominant, well-documented roles in the condensed phase, 2 $^1A_g \leftarrow 1$ ^1A_g transitions of several model polyenes. Finally, the almost identical lifetimes of the peaks assigned to FO1 and FO2 (see Table I) confirm that they belong to the same transition of the same molecule and that they cannot be due to different conformers or isomers of decatetraene.

Further analysis of the spectrum suggests that the peak 259 cm^{-1} above FO1 should be assigned to a second Herzberg–Teller false origin (FO3). This (like FO2) appears as a single, sharp peak and thus cannot be easily reconciled with an a_g vibration built on the FO1 triplet. This most likely is a counterpart of the 463 cm^{-1} b_u mode observed in the 2 $^1A_g \leftarrow 1$ ^1A_g spectrum of condensed-phase octatetraene[46]

and predicted at 282 cm^{-1} in ground-state decapentaene.[47] Progressions built on this mode appear at higher frequencies (see Table I) and contribute to the spectral congestion for vibronic energies > 400 cm^{-1}.

Analysis of the remainder of the 2 $^1A_g \leftarrow 1$ ^1A_g excitation spectrum primarily rests on numerology and the characteristic triplet and singlet structure of progressions built on the two types of false origins. In order to simplify the presentation of the spectrum, only the maximum of each of the "triplets" is given in Table I. We first focus on the low-energy region (0–800 cm^{-1}). As shown in the table, almost all of the prominent, low-frequency vibronic features seen in Figs. 4 and 5 can be assigned to simple combinations of the following frequencies: 139, 203, 223, 329, and 416 cm^{-1}. The fact that these frequencies appear both as single and double quanta indicates a_g symmetries for these vibrations. (This analysis assumes that decatetraene retains its C_{2h} symmetry in the 2 ^1A_g state.) However, normal-mode calculations suggest that some of these frequencies are double quanta or combination bands of nontotally symmetric fundamentals (a_u or b_g). Two of these modes are most likely the 2 ^1A_g counterparts of the a_g vibrations that are active in the 1 $^1B_u \leftarrow 1$ ^1A_g absorption (132 and 273 cm^{-1}) (Ref. 15) and in the 1 $^1B_u \rightarrow 1$ ^1A_g emission (~ 150 and 290 cm^{-1}). Gavin and Rice[47] predict a_g in-plane bends of 158 and 299 cm^{-1} for ground-state decapentaene, within the range of vibrations we have observed for isolated decatetraene. (Decapentaene and decatetraene should have comparable low-frequency, skeletal bending modes due to similar reduced masses and force constants.) However, the next a_g vibration is calculated at 425 cm^{-1} (535 cm^{-1} in octatetraene).[47–49] This strongly implies that at least two of the low-frequency vibrations given above involve nontotally symmetric vibrations. There are several low-frequency, a_u and b_g candidates, including modes that involve methyl torsions as well as torsions about carbon–carbon single and double bonds. However, positive identification of these vibrations (as well as many of the low-frequency a_g and b_u modes) awaits calculation of the decatetraene 1 ^1A_g and 2 ^1A_g normal modes.

It should be stressed that the analysis given in Table I uses the *minimum* number of low-frequency modes to account for the bulk of the $S_1 \leftarrow S_0$ excitation vibronic intensity. The triplet fine structure of progressions built on FO1, the number of low-frequency modes, and the approximate coincidence between FO1 + 203 cm^{-1} and FO2 + 139 cm^{-1} contribute to a rather complex spectrum. The complexity and broadness of the spectrum given in Fig. 5 does not preclude the existence of other low-frequency (300–800 cm^{-1}) modes that could not easily be distinguished from combination bands of the modes listed above. These modes would add to the list of low-frequency, nontotally symmetric vibrations that are active in the spectrum.

Finally, we consider vibronic bands 800–1350 cm^{-1} above the 2 $^1A_g \leftarrow 1$ ^1A_g origin. As shown in Figs. 4 and 5, there are several sharp features in the spectrum that are most plausibly assigned to fundamentals. Methyl rocking modes (both a_g and b_u) and additional in-plane, b_u skeletal bending modes are logical candidates for this frequency range,

though it is not possible to make specific assignments at present. The totally symmetric, carbon–carbon, single-bond-stretching mode appears both as a triplet (FO1 + 1232 cm^{-1}) and as a singlet (FO2 + 1232 cm^{-1}). Carbon–carbon stretching modes are a well-known signature of polyene spectroscopy and are a consequence of the rearrangement of π bond orders upon electronic excitation. On the other hand, methyl rocking vibrations typically do not play a significant role in the vibronic spectra of polyenes. Their strong activity in the 2 $^1A_g \leftarrow 1$ ^1A_g spectrum of decatetraene reinforces our conclusion that the torsional motions of the methyl groups promote coupling between the 2 ^1A_g and 1 ^1B_u states and suggests distortion along these coordinates in 2 ^1A_g.

D. Fluorescence lifetimes of 2 ^1A_g vibronic levels in isolated decatetraene

Fluorescence lifetimes for individual vibronic levels are listed in Table I and plotted in Fig. 4. Lifetimes of the false origins are comparable to those obtained for vibrationally relaxed molecules in argon clusters (~ 360 ns) and again indicate both relatively high fluorescence quantum yields and weak, symmetry-forbidden transitions, as expected for *all-trans*-decatetraene. The relatively smooth falloff in lifetimes further indicates that all of these vibronic features are associated with the same electronic transition and eliminates the possibility that some parts of the spectrum might be assigned to conformers or isomers without inversion centers.

The emission lifetimes of individual 2 ^1A_g vibronic levels decrease with increasing energy above FO1. This is most easily explained by an increase in vibronic coupling as the $S_2 - S_1$ energy difference decreases. Intensity borrowing between the 2 $^1A_g \leftarrow 1$ ^1A_g and 1 $^1B_u \leftarrow 1$ ^1A_g transition is well documented for polyenes in solution,[1,64] and has been used to explain the level-dependent fluorescence lifetimes of diphenylbutadiene and diphenylhexatriene in supersonic expansions.[28,29] The absorption strength of the 2 $^1A_g \leftarrow 1$ ^1A_g transition thus should increase inversely with the square of the energy separation (ΔE) between the 2 ^1A_g and 1 ^1B_u states. As seen in Fig. 4, the 2 ^1A_g vibronic lifetimes of decatetraene are well accounted for by this simple model [$\tau = (\Delta E/\Gamma)^2$, where Γ is a measure of vibronic coupling]. The fit indicated in Fig. 4 gives a Γ of 7.6×10^{13} cm^{-2} s^{-1} which is comparable to Γ's obtained from analysis of the solvent-dependent lifetimes of diphenylhexatriene and *all-trans* retinol.[64] Assuming a 1 $^1B_u \leftarrow 1$ ^1A_g oscillator strength of 1.00 and taking an average frequency of the 2 $^1A_g \leftarrow 1$ ^1A_g transition as 29 000 cm^{-1} yields a vibronic coupling matrix element of 560 cm^{-1}. (Compare 555 and 149 cm^{-1} in diphenylhexatriene and retinol.[64])

Considering the above arguments, it perhaps is surprising that the free molecule and Ar cluster lifetimes are so similar. The smaller $S_2 - S_1$ energy difference for the Ar clusters (4300 cm^{-1} vs 5800 cm^{-1} for the free molecule) should almost double the fluorescence decay rate. The comparable fluorescence lifetimes of the clusters and isolated decatetraene is most likely due to higher fluorescence yields in the clusters. This is not unexpected given the expected

sensitivity of nonradiative decay rates on the solvent environment and internal energy of the decatetraene. This also suggests that the fluorescence yield of free decatetraene is less than unity, which might help explain the difference between the ~ 340 ns free-molecule lifetime and the 500 ns lifetime predicted from lifetime and quantum yield measurements of decatetraene in room-temperature solution.[5]

IV. SUMMARY AND CONCLUSION

The discovery of 1 $^1B_u \rightarrow 1$ ^1A_g and 2 $^1A_g \rightarrow 1$ ^1A_g emissions in gaseous tetraenes and pentaenes[15] means that both the 1 ^1B_u and the 2 ^1A_g states of isolated polyenes can be investigated using fluorescence excitation techniques. Measurements on decatetraene have provided the first detailed look at the vibronic structure and kinetics of the 2 ^1A_g state of an *all-trans* polyene under isolated molecule conditions. The ability of polyenes to undergo large-amplitude motions is reflected in the important roles played by low-frequency vibrations in the electronic spectra. This is particularly evident in the weak, symmetry-forbidden 2 $^1A_g \leftarrow 1$ ^1A_g transition which is dominated by progressions of low-frequency modes. Normal coordinate calculations indicate that some of these low-frequency vibrations may involve out-of-plane modes (a_u and b_g) which involve carbon–carbon torsion internal coordinates. Such modes are of obvious interest in understanding the *trans*↔*cis* photochemistries of polyene systems. The low-frequency progressions are built on false origins that can, in turn, be assigned to low-frequency (~ 65 and 265 cm^{-1}) b_u promoting modes which mix the 2 ^1A_g and 1 ^1B_u states. In addition, it appears that the torsional and rocking motions of the terminal methyl groups also are strongly coupled to the electronic motion. The vibronic states have long fluorescence lifetimes (~ 350 ns for the false origins) as expected for the symmetry-forbidden, vibronically induced, 2 $^1A_g \rightarrow 1$ ^1A_g transition of an *all-trans* polyene.

The flexibility of polyenes distinguishes them from aromatic systems and clearly is an important factor in their unique ground- and excited-state chemistries. However, the important role of large-amplitude motions has not previously been observed in the electronic spectroscopy of polyenes in solutions and crystals where lattice and phonon modes tend to obscure rotations and low-frequency vibrations. The connection between methyl torsions and the coupling between electronic states also has not been noted in polyene spectroscopy, though there is precedence for this observation in the spectroscopy of small molecules such as biacetyl[65] and in several methyl-substituted benzenes.[50–53] Coupling of the methyl torsions to carbon–carbon torsions and other low-frequency modes appears to be strong and perhaps plays an important role in accelerating cis-trans isomerization in these model polyene systems.

The free-jet, two-photon, $S_0 \rightarrow S_1$ fluorescence excitation spectrum and $S_1 \rightarrow S_0$ fluorescence spectra from single vibronic levels of 2 ^1A_g would be useful in confirming our spectral assignments as well as providing insights on the role of intramolecular vibrational redistribution (IVR) in these

systems. Extension of our experiments to nonatetraene and octatetraene is in progress and should lead to a better understanding of the role of substituents and the effect of reduced symmetry on the spectroscopy and dynamics of these molecules. The increase in the ratio of $S_1 \rightarrow S_0/S_2 \rightarrow S_0$ fluorescence intensities in gaseous pentaenes indicates that fluorescence and fluorescence excitation techniques should allow similarly detailed studies of the $2\,^1A_g$ states of longer polyenes in supersonic molecular jets, both as isolated molecules and in solvent clusters.

The free-jet experiments described in this paper also raise several theoretical issues. For example, normal coordinate calculations on the $1\,^1A_g$, $2\,^1A_g$, and $1\,^1B_u$ states of decatetraene, nonatetraene, and related molecules would greatly facilitate the analysis of the vibronic spectra and lead to a better understanding of the low-frequency vibrations. Estimates of barriers to internal rotation and *cis-trans* isomerization in the ground and excited states of these molecules also are of considerable interest. The apparently strong interactions between the π electrons and the methyl rotations clearly deserve further study. Any accounting of the triplet pattern observed for the false origin (Fig. 5) will require use of the full molecular symmetry group,[66] and in the case of decatetraene should consider possible couplings between the two methyl rotors.[67,68] The distinctive structure and splittings of these peaks should provide useful benchmarks for evaluating theoretical descriptions of the $2\,^1A_g$ states in model polyenes.

ACKNOWLEDGMENTS

[1] B. S. Hudson, B. E. Kohler, and K. Schulten, in *Excited States*, edited by E. C. Lim (Academic, New York, 1982), Vol. 6, p. 1.

[2] R. B. Woodward and R. Hoffman, *The Conservation of Orbital Symmetry* (Verlag Chemie, Weinheim, 1970).

[3] K. Fukui, Acc. Chem. Res. 4, 57 (1971).

[4] R. M. Gavin, Jr., C. Weisman, J. K. McVey, and S. A. Rice, J. Chem. Phys. 68, 522 (1978).

[5] J. R. Andrews and B. S. Hudson, Chem. Phys. Lett. 57, 600 (1978).

[6] M. F. Granville, G. R. Holtom, B. E. Kohler, R. L. Christensen, and D'Amico, J. Chem. Phys. 70, 593 (1979).

[7] K. L. D'Amico, C. Manos, and R. L. Christensen, J. Am. Chem. Soc. 102, 1777 (1980).

[8] L. A. Heimbrook, J. E. Kenny, B. E. Kohler, and G. W. Scott, J. Chem. Phys. 75, 4338 (1981).

[9] D. G. Leopold, V. Vaida, and M. F. Granville, J. Chem. Phys. 81, 4210 (1984).

[10] D. G. Leopold, R. D. Pendley, J. L. Roebber, R. J. Hemley, and V. J. Vaida, Chem. Phys. 81, 4218 (1984).

[11] L. A. Heimbrook, B. E. Kohler, and I. J. Levy, J. Chem. Phys. 81, 1592 (1984).

[12] R. Snyder, E. Arvidson, C. Foote, L. Harrigan, and R. L. Christensen, J. Am. Chem. Soc. 107, 4117 (1985).

[13] J. H. Simpson, L. McLaughlin, D. S. Smith, and R. L. Christensen, J. Chem. Phys. 87, 3360 (1987).

[14] B. Kohler, C. Spangler, and C. J. Westerfield, J. Chem. Phys. 89, 5422 (1988).

[15] W. G. Bouwman, A. C. Jones, D. Phillips, P. Thibodeau, C. Friel, and R. L. Christensen, J. Phys. Chem. 94, 7429 (1990).

[16] S. A. Cosgrove, M. A. Guite, T. B. Burnell, and R. L. Christensen, J. Phys. Chem. 94, 8118 (1990).

[17] F. Zerbetto and M. Z. Zgierski, J. Chem. Phys. 93, 1235 (1990).

[18] M. Aoyagi, Y. Osamura, and S. Iwata, J. Chem. Phys. 83, 1140 (1985).

[19] L. D. Ziegler and B. S. Hudson, J. Chem. Phys. 79, 1197 (1983); R. J. Sension, L. Mayne, and B. Hudson, J. Am. Chem. Soc. 109, 5036 (1987).

[20] V. Bonacic-Koutecky, M. Persico, D. Dohnert, and A. Sevin, J. Am. Chem. Soc. 104, 6900 (1982).

[21] G. J. Dormans, G. C. Groenenboom, and H. M. Buck, J. Chem. Phys. 86, 4895 (1987).

[22] A. B. Myers and K. S. Pranata, J. Phys. Chem. 93, 5079 (1989).

[23] X. Ci, M. A. Pereira, and A. B. Myers, J. Chem. Phys. 92, 4708 (1990).

[24] M. O. Trulson and R. A. Mathies, J. Chem. Phys. 94, 5741 (1990).

[25] R. R. Chadwick, D. P. Gerrity, and B. S. Hudson, Chem. Phys. Lett. 115, 24 (1985).

[26] M. F. Granville, G. R. Holtom, and B. E. Kohler, Proc. Natl. Acad. Sci, U.S.A. 77, 31 (1980).

[27] J. R. Ackerman and B. E. Kohler, J. Am. Chem. Soc. 106, 3681 (1984).

[28] L. A. Heimbook, B. E. Kohler, and T. A. Spiglanin, Proc. Natl. Acad. Sci. U.S.A. 80, 4580 (1983).

[29] B. E. Kohler and T. A. Spiglanin, J. Chem. Phys. 80, 5465 (1984).

[30] J. A. Syage, P. M. Felker, and A. H. Zewail, J. Chem. Phys. 81, 4685 (1984).

[31] J. A. Syage, P. M. Felker, and A. H. Zewail, J. Chem. Phys. 81, 4706 (1984).

[32] A. Amirav and J. Jortner, Chem. Phys. Lett. 95, 295 (1983).

[33] J. Troe, A. Amirav, and J. Jortner, Chem. Phys. Lett. 115, 245 (1985).

[34] A. Amirav, M. Sonnenschein, and J. Jortner, Chem. Phys. 102, 305 (1986).

[35] J. F. Shepanski, B. W. Keelan, and A. H. Zewail, Chem. Phys. Lett. 103, 9 (1983).

[36] J. S. Horwitz, B. E. Kohler, and T. A. Spiglanin, J. Chem. Phys. 83, 2186 (1985).

[37] J. S. Horwitz, B. E. Kohler, and T. A. Spiglanin, J. Phys. Chem. 89, 1574 (1985).

[38] T. Itoh and B. E. Kohler, J. Phys. Chem. 92, 1807 (1988).

[39] H. Petek, Y. Fujiwara, D. Kim, and K. Yoshihara, J. Am. Chem. Soc. 110, 6269 (1988).

[40] J. H. Frederick, Y. Fujiwara, J. H. Penn, K. Yoshihara, and H. Petek, J. Phys. Chem. 95, 2845 (1991).

[41] J. F. Pfanstiel. B. B. Champagne, W. A. Majewski, D. F. Plusquellic, and D. W. Pratt, Science 245, 736 (1989).

[42] B. B. Champagne, J. F. Pfanstiel, D. F. Plusquellic, D. W. Pratt, W. M. van Herpen, and W. L. Meerts, J. Phys. Chem. 94, 6 (1990).

[43] W. J. Buma, B. E. Kohler, and K. Song, J. Chem. Phys. 92, 4622 (1990); 94, 4691 (1991); 94, 6367 (1991).

[44] R. Howell, H. Petek, D. Phillips, and K. Yoshihara, Chem. Phys. Lett. (submitted).

[45] R. L. Christensen and B. E. Kohler, J. Chem. Phys. 63, 1837 (1975).

[46] M. F. Granville, G. R. Holtom, and B. E. Kohler, J. Chem. Phys. 72, 4671 (1980).

[47] R. M. Gavin, Jr. and S. A. Rice, J. Chem. Phys. 55, 2675 (1971).

[48] B. S. Hudson and J. R. Andrews, Chem. Phys. Lett. 63, 493 (1979).

[49] A. C. Lasaga, R. J. Aerni, and M. Karplus, J. Chem. Phys. 73, 5230 (1980); H. Yoshida and M. Tasumi, *ibid.* 89, 2803 (1988).

[50] J. Murakami, M. Ito, and K. Kaya, Chem. Phys. Lett. 80, 203 (1981).

[51] M. Ito, J. Phys. Chem. 91, 517 (1987).

[52] M. Ito, T. Ebata, and N. Mikami, Annu. Rev. Phys. Chem. 39, 123 (1988).

[53] P. J. Breen, J. A. Warren, E. R. Bernstein, and J. I. Seeman, J. Chem. Phys. 87, 1917 (1987).

[54] K. Okuyama, N. Mikami, and M. Ito, J. Phys. Chem. 89, 5617 (1985).

[55] W. H. Flygare, *Molecular Structure and Dynamics* (Prentice-Hall, Englewood Cliffs, NJ, 1978), pp. 128–135.

[56] E. Hirota, J. Chem. Phys. 45, 1984 (1966).

[57] D. R. Lide, Jr. and M. Jen, J. Chem. Phys. **40**, 252 (1964).

[58] S. L. Hsu and W. H. Flygare, J. Mol. Spectrosc. **32**, 375 (1969).

[59] U. Dinur, R. J. Hemley, and M. Karplus, J. Phys. Chem. **87**, 924 (1983).

[60] R. J. Hemley, B. Brooks, and M. Karplus, J. Chem. Phys. **85**, 6550 (1986).

[61] R. J. Hemley, A. C. Lasaga, V. Vaida, and M. Karplus, J. Phys. Chem. **92**, 945 (1988).

[62] M. Aoyagi, I. Ohmine, and B. Kohler, J. Phys. Chem. **94**, 3922 (1990).

[63] A. E. Dorigo, D. W. Pratt, and K. N. Houk, J. Am. Chem. Soc. **109**, 6591 (1987).

[64] J. R. Andrews and B. S. Hudson, J. Chem. Phys. **68**, 4587 (1978).

[65] L. Spangler and D. Pratt, J. Chem. Phys. **84**, 4789 (1986).

[66] H. C. Longuet-Higgins, Mol. Phys. **6**, 445 (1963).

[67] P. Groner and J. R. Durig, J. Chem. Phys. **66**, 1856 (1977).

[68] P. Groner, J. F. Sullivan, and J. R. Durig, *Vibrational Spectra and Structure*, edited by J. R. Durig (Elsevier, New York, 1981), Vol. 9, p. 405.